# Modeling, Design and Implementation of Electronic controller for BLDC MACHINE

*A Project Report*

*submitted by*

**PENUMUDI RAVITEJA**

*in partial fulfilment of the requirements*
*for the award of the degree of*

**MASTER OF TECHNOLOGY**


**DEPARTMENT OF ELECTRICAL ENGINEERING**
**INDIAN INSTITUTE OF TECHNOLOGY MADRAS.**

**MAY 2013**

# THESIS CERTIFICATE

This is to certify that the thesis titled **SPEED CONTROL OF BLDC MOTOR**, submitted by **PENUMUDI RAVITEJA**, to the Indian Institute of Technology, Madras, for the award of the degree of **MASTER OF TECHNOLOGY**, is a bona fide record of the research work done by him under our supervision. The contents of this thesis, in full or in parts, have not been submitted to any other Institute or University for the award of any degree or diploma.

**Dr.N.Lakshmi Narasamma**
Assistant Professor
Dept. of Electrical Engineering
IIT-Madras, 600 036

Place: Chennai

May 22, 2013

# ACKNOWLEDGEMENTS

I consider it an honour to work with Dr.N.Lakshmi Narasamma, my guide who made this thesis possible.

I would like to thank lab incharges for providing equipment each and everytime when needed.

I owe my deepest gratitude to my fellow labmates who made the lab environment conducive to work.

I thank my parents for their unconditional support throughtout my life.

Above all, I thank God who helped me in everything.

# ABSTRACT

KEYWORDS: BLDC ; Speed control; Simulation; Hardware.

BLDC motors are one of the motors rapidly gaining popularity. It has several advantages over brushed DC motor and Induction motor. BLDC motors are used in industries such as Appliances, Automotive, Aerospace, Consumer, Medical, Industrial Automation Equipment and Instrumentation. Many applications require control of speed. This project emphasises on speed control of BLDC motor. Speed of BLDC motor is controlled in following ways.

1. Pulse-width modulated(PWM) control
2. DC-Link voltage control
3. Hysteresis band control

In this thesis design and implementation of PWM control and DC-Link voltage control method of speed control of BLDC motor are presented.

# TABLE OF CONTENTS

# LIST OF TABLES

# LIST OF FIGURES

# CHAPTER 1

# INTRODUCTION

Adjustable speed drives are gaining more importance than fixed-speed drives. Three common reasons for preferring an adjustable speed drive are

1. energy saving
2. velocity or position control and
3. amelioration of transients

It is the motor that determines the charateristics of a drive, and it also determines the requirements on power semiconductors, the converter circuit, and the control[1]. The availability of modern permanent magnets(PM) with considerable energy density led to development of dc machines with PM field excitation. Introduction of permanent magnets to replace electro magnets resulted in compact dc machines. The synchronous machine with its conventional field excitation in the rotor is replaced by PM ecxitation. With the advent of switching power transistor & silicon-controlled rectifier the replacement of mechanical commutation with electrical commutation in the form of inverter was achieved. These led to development of PM synchronous and brushless dc machines. The smaller the motor, the more sense it makes to use permanent magnets for excitation[3]. Brushless DC(BLDC) motor is a synchronous electric motor powered by a direct current. As the name implies, the BLDC Motor does not operate using brushes; rather it operates with a controller via electronic commutation. In 1-10 kW range BLDC motor is preferred to induction motor[1]. Above 10 kW, induction motor is preferred[1]. Below 10 kW range, the PM motor has better efficiency, torque per ampere and effective power factor. Moreover for PM BLDC motor, the power winding is on the stator where its heat can be removed more easily, while the rotor losses are extremely small. These factors combine to keep the torque/inertia ratio high in small motors[1].

The PM BLDC motor has permanent magnets instead of a field winding. Field control is again sacrificed for the elimination of brushes, sliprings and field copper losses.

## 1.1 Permanent magnet versus Electromagnetic excitation

A permanent magnet is an object made from a material that is magnetized and creates its own persistent magnetic field. It always has a magnetic field and will display a magnetic behavior at all times. An electromagnet is made from a coil of wire which acts as a magnet when an electric current passes through it. Often an electromagnet is wrapped around a core of ferromagnetic material like steel, which enhances the magnetic field produced by the coil.

As the geometric size is decreased, the cross-sectional area available for copper conductors decreases with the square of linear dimension, but the need for m.m.f decreases only with linear dimension being primarily determined by the length of air-gap. As the motor size is further decreased, the airgap length reaches a minimum value below which the m.m.f requirement decreases only slowly while the copper area continues to decrease with the squared linear dimension[1]. The loss-free excitation provided by permanent magnents increases in relative value as the motor size is decreased.

In larger motors magnets can help to improve the efficiency by eliminating the losses associated with electromagnetic field windings. At the same time the required volume of magnets with adequate properties increases with the motor size to the point where PM excitation is too expensive.

Another reason why permanent magnets are not suitable for larger machines is that these machines often need a constant-power characteristic at higher speeds or atleast field-weakening capability but field-weakening is not possible with PM motors[1].

There is no fixed power level below which permanent-magnet excitation becomes advantageous, but it is possible to determine the excitation penalty in ways which indicate roughly where the breakpoint lies. Table 1.1 and Table 1.2 lists out the comparison between BLDC motor, DC motor and Induction motor[4]. The construction of BLDC motor is explained in the next section.

Table 1.1: Comparison of BLDC and DC motor

| *Feature* | *BLDC motor* | *DC motor* |
|---|---|---|
| Commutation | Electronic commutation. | Brushed commutation. |
| Maintenance | Less-due to absence of brushes. | Periodic maintenance is required. |
| Rotor inertia | Low-because of permanent magnets on rotor which improves dynamic response. | High-which limits dynamic response. |
| Speed range | Higher-No mechanical limitation imposed by brushes/commutator. | Lower-mechanical limitation by the brushes. |
| Control | Complex and expensive. | Simple and inexpensive. |
| Cost | High-since it has permanent magnets | Low |
| Life | Longer. | Shorter. |
| Efficiency | High-due to no voltage drop across brushes. | Low. |

Table 1.2: Comparison of BLDC and Induction motor

| *Feature* | *BLDC motor* | *Induction motor* |
|---|---|---|
| Starting current | Rated-No special starter circuit required. | Upto 7 times of rated current. |
| Speed-Torque characteristics | Flat-Enables operation at all speeds with rated load. | Non-linear-because lower torque at lower speeds. |
| Rotor inertia | Low-because of permanent magnets on rotor which improves dynamic response. | High-which limits dynamic response. |
| Slip | There is no slip between stator and rotor frequency. | The rotor runs at a lower frequency than stator by slip frequency and slip increases with load on the motor. |

## 1.2 Construction of BLDC motor

The motor has 3-phase delta connected or star connected stator and the rotor with permanent magnets.

STATOR: The stator of a BLDC motor consists of stacked steel laminations with windings placed in the slots that are axially cut along the inner periphery. The stator resembles that of an induction motor; however, the windings are distributed in a different manner. Most BLDC motors have three stator windings connected in star fashion or delta connection. Each of these windings are constructed with numerous coils interconnected to form a winding. One or more coils are placed in the slots and they are interconnected to make a winding. Each of these windings are distributed over the stator periphery to form an even numbers of poles. There are two types of stator windings variants: trapezoidal and sinusoidal motors. This differentiation is made on the basis of the interconnection of coils in the stator windings to give the different types of back electromotive force (emf). The trapezoidal motor gives a back emf in trapezoidal fashion and the sinusoidal motors back emf is sinusoidal, as shown in Figures 1.1 and 1.2.

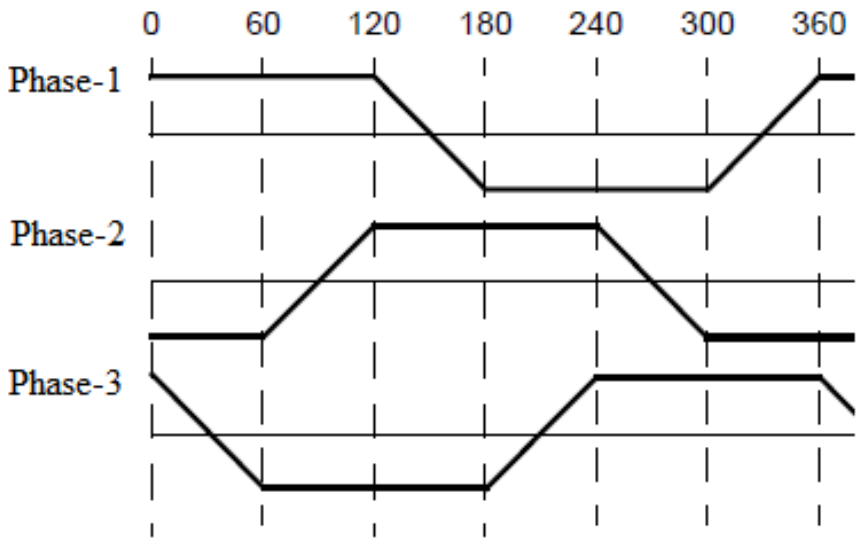


Figure 1.1: Trapezoidal back emf

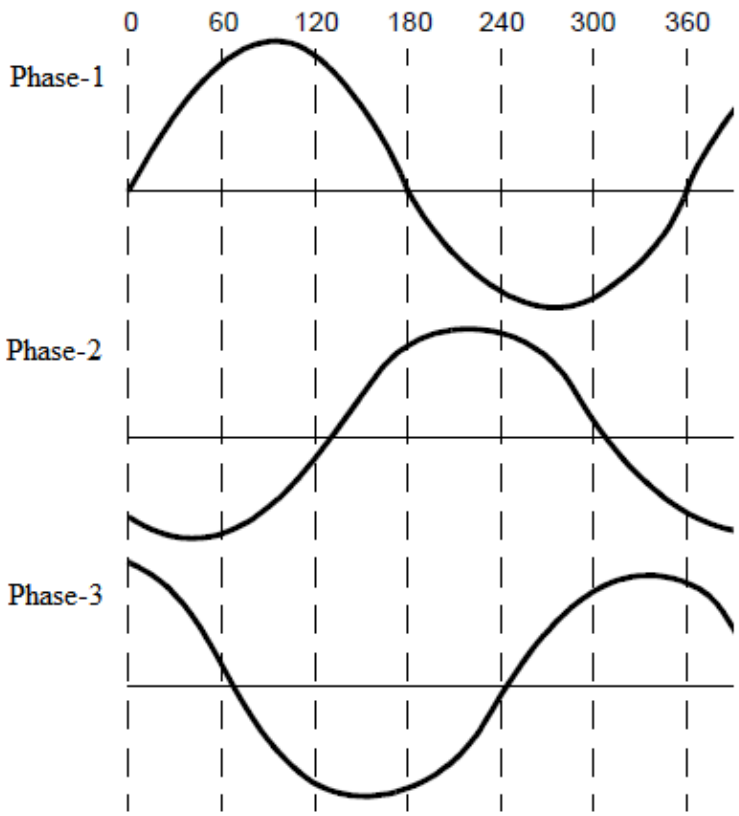


Figure 1.2: Sinusoidal back emf

In addition to the back emf, the phase current also has trapezoidal and sinusoidal variations in the respective types of motor. This makes the torque output by a sinusoidal motor smoother than that of a trapezoidal motor. However, this comes with an extra cost, as the sinusoidal motors take extra winding interconnections because of the coils distribution on the stator periphery, thereby increasing the copper intake by the stator windings.

ROTOR: The rotor is made of permanent magnets. Permanent magnet synchronous machines can be broadly classified on the basis of the direction of field flux.

1. Radial field: the flux direction is along the radius of the machine.
2. Axial field: the flux direction is parallel to the rotor shaft.

The magnets can be placed in many ways on the rotor. The high-power-density synchronous machines have surface PM's with radial orientation intended generally for low speed applications whereas interior-magnet version is used for high speed applications[2]. The function of the magnet is same in both the brushless motor and dc

commutator motor. In both the cases the airgap flux is ideally fixed by the magnets and little affected by armature current.

HALL SENSORS: The commutation of a BLDC motor is controlled electronically unlike DC motor . To rotate the BLDC motor, the stator windings should be energized in a sequence. It is important to know the rotor position in order to understand which winding will be energized following the energizing sequence. Rotor position is sensed using Hall effect sensors embedded into the stator. Most BLDC motors have three Hall sensors embedded into the stator on the non-driving end of the motor. The transverse section of BLDC is shown in Figure 1.3[4].

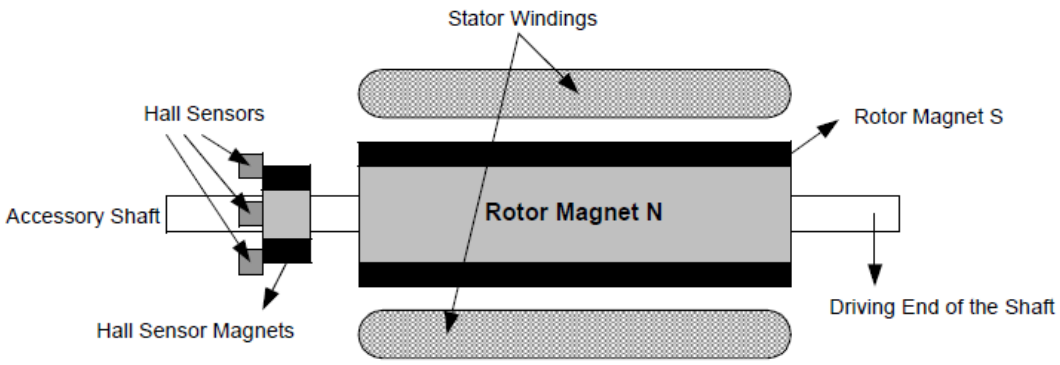


Figure 1.3: Transverse section of BLDC motor

Whenever the rotor magnetic poles pass near the Hall sensors, they give a high or low signal, indicating the N or S pole is passing near the sensors. Based on the combination of these three Hall sensor signals, the exact sequence of commutation can be determined[4]. The following section explains the operating principle of BLDC motor.

## 1.3 Operating principle of BLDC motor

For analysis delta connected bldc motor is considered. The 3-phase delta connected stator windings of the BLDC motor is shown in Figure 1.4.

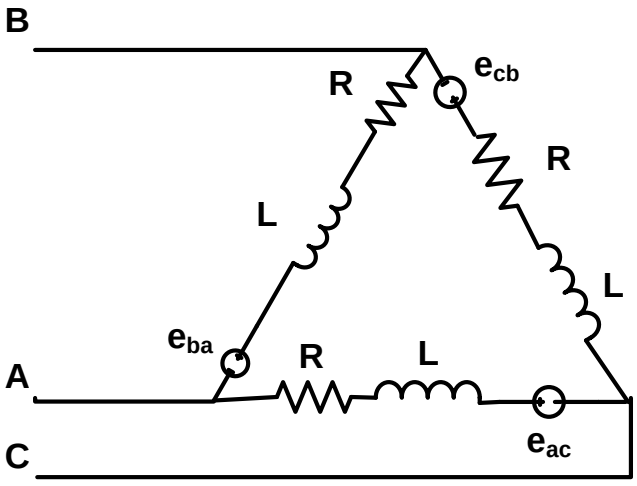


Figure 1.4: Electrical equivalent of stator windings of BLDC motor

R and L are the stator resistance and inductance per phase. $e_{ba}$, $e_{cb}$ and $e_{ac}$ are emf′s induced in the stator due to permanent magnets. $H_b$, $H_c$ and $H_a$ are the hall sensor signals corresponding to $e_{ba}$, $e_{cb}$ and $e_{ac}$ respectively are shown in Figure 1.5 w.r.t rotor position.

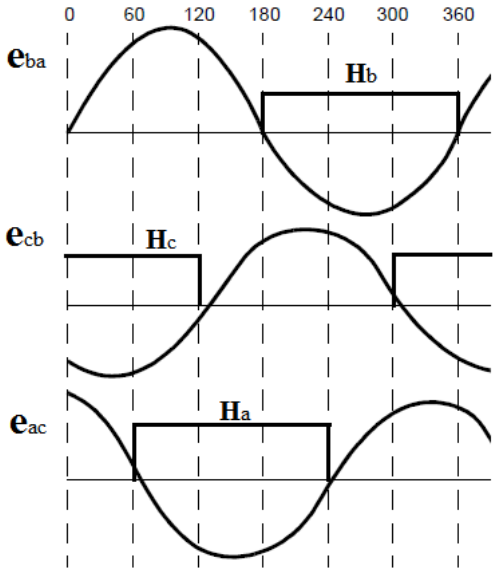


Figure 1.5: Back emf and Hallsensor signals of BLDC motor

Based on the Hall sensor signals, commutation sequence is derived which is shown in Table 1.3 such that during each commutation sequence full dc voltage is applied to one winding and half the voltage is applied to each of the other two windings. Torque is produced because of the interaction between the magnetic field generated by the stator

coils and the permanent magnets. Block diagram of BLDC drive is shown in Figure 1.6.

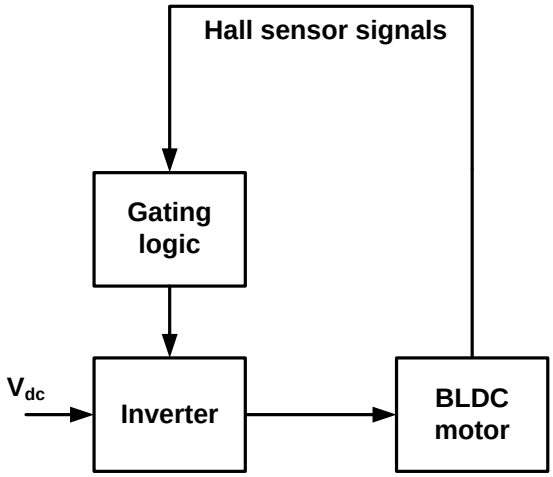


Figure 1.6: Block diagram of bldc drive

Delta connected BLDC motor driven by inverter is shown in Figure1.7.

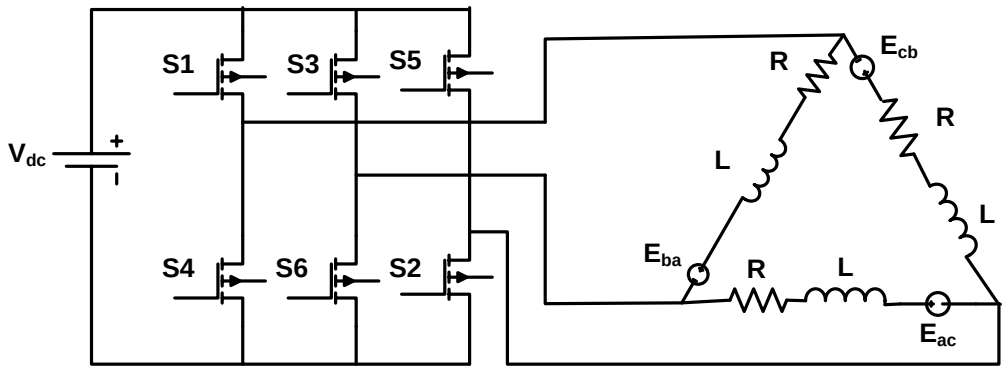


Figure 1.7: Delta connected BLDC with inverter

Table 1.3 shows the switching sequence that should be followed w.r.t Hall sensors. Every 60 electrical degrees of rotation of rotor, one of the Hall sensors changes the state. So it takes six steps to complete an electrical cycle. From Table 1.3, equivalent circuit for $60^{\circ}$ is shown in Figure 1.8.

Table 1.3: Commutation sequence derived from hall sensors

| *Rotor position* | $H_a$ | $H_b$ | $H_c$ | $S1$ | $S2$ | $S3$ | $S4$ | $S5$ | $S6$ | *Phase to which full voltage is applied* |
|---|---|---|---|---|---|---|---|---|---|---|
| 0°-60° | 0 | 0 | 1 | 1 | 1 | 0 | 0 | 0 | 0 | BC |
| 60°-120° | 1 | 0 | 1 | 1 | 0 | 0 | 0 | 0 | 1 | BA |
| 120°-180° | 1 | 0 | 0 | 0 | 0 | 0 | 0 | 1 | 1 | CA |
| 180°-240° | 1 | 1 | 0 | 0 | 1 | 0 | 1 | 1 | 0 | CB |
| 240°-300° | 0 | 1 | 0 | 0 | 0 | 1 | 1 | 0 | 0 | AB |
| 300°-360° | 0 | 1 | 1 | 0 | 1 | 1 | 0 | 0 | 0 | AC |

For the interval 0°- 60°, switches $S1$ and$S2$ are ON which can be seen from the Table 1.3. The equivalent circuit of the motor is shown in Figure 1.8 for the duration 0°- 60°. Similarly for all the other intervals equivalent circuit may be derived.

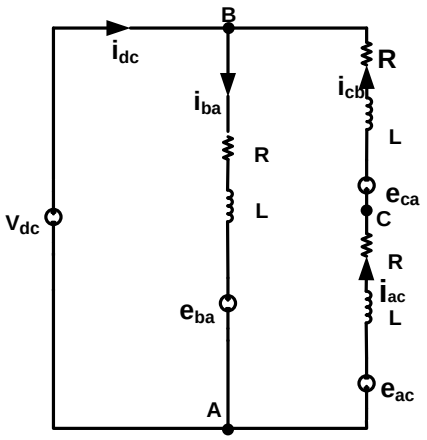


Figure 1.8: Equivalent circuit for 0°- 60°

## 1.4 Speed control

Speed of BLDC motor is controlled by PWM control, Hysterisis control and DC-Link voltage control. These control methodologies are explained below.

**PWM control**

In PWM control the motor is turned ON and OFF at high rate. The frequency of operation is fixed but the ON and OFF times are varied which depend on control

error. The switching frequency is in the range of few tens of kHz and the fact that switching frequency is fixed, makes filtering of noise easier.

**Hysteresis control**

In Hysteresis control the value of the controlled variable is forced to stay within certain limits. For example if the control variable is motor speed, the motor is turned off if the speed reaches above the reference speed and turned on again if the speed falls below the certain speed below the reference speed. The drawback of this control technique is high and uncontrolled switching frequencies when a narrow hysteresis band is used and large ripples when the hysteresis band is wider[3].

**DC-Link voltage control**

DC-Link voltage is varied by using DC-DC converter. In this mode of control switching losses are reduced as only one switch need to chopped but the torque ripple is high compared to PWM control.

This thesis presents simulation of delta connected BLDC motor in PWM control & DC-Link voltage control mode. Hardware implementation is presented for PWM mode of control.

## 1.5 Organisation of thesis

Chapter 2 deals with Modeling of BLDC motor, design of speed controller & current controller and simulation results.
Chapter 3 covers Hardware implementation and results.
Chapter 4 presents the conclusion.

# CHAPTER 2

# MODELING AND CONTROL

## 2.1 Description

BLDC motor is similar to DC motor in operation. The model of BLDC motor is similar to that of DC machine. Modeling is presented in the following section.

## 2.2 Modeling of BLDC machine

The dynamic and steady state equations of BLDC motor are derived from the equivalent circuit which is shown in Figure 2.1 which is valid for 0°- 60° as seen from Table 1.3.

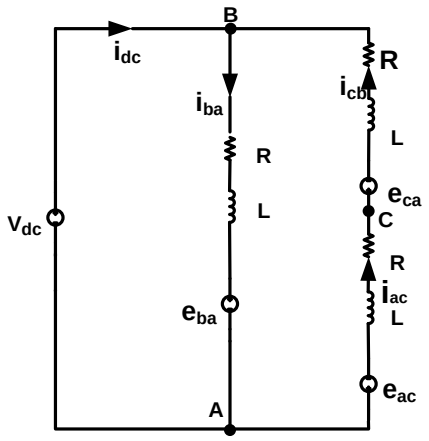


Figure 2.1: Equivalent circuit for 0°- 60°

### 2.2.1 Dynamic model

Electrical equations:

$$v_{ba} = Ri_{ba} + L\frac{di_{ba}}{dt} + e_{ba} \tag{2.1}$$

$$v_{cb} = Ri_{cb} + L\frac{di_{cb}}{dt} + e_{cb} \tag{2.2}$$

$$v_{ac} = Ri_{ac} + L\frac{di_{ac}}{dt} + e_{ac} \tag{2.3}$$

where $v_{ba}$- instantaneous voltage across phase BA. Similarly $v_{cb}$ and $v_{ac}$.

$i_{ba}$- instantaneous current through phase BA. Similarly $i_{cb}$ and $i_{ac}$.

Back emf equations:

$$e_{ba} = k_b \omega_m f(\theta_e) \tag{2.4}$$

$$e_{cb} = k_b \omega_m f(\theta_e - 120^\circ) \tag{2.5}$$

$$e_{ac} = k_b \omega_m f(\theta_e + 120^\circ) \tag{2.6}$$

where

$k_t$- torque constant

$k_b$- back emf constant; $k_t = k_b$ from motor parameters given in appendix A.

$\omega_m$- rotor speed

$\theta_e$- rotor electrical angle

$f(\theta_e) = sin\theta_e$

Mechanical equations:

$$T_e = T_l + J\frac{d\omega_m}{dt} + B\omega_m \tag{2.7}$$

$$T_e = k_t\{f(\theta_e)i_{ba} + f(\theta_e - 120^\circ)i_{cb} + f(\theta_e + 120^\circ)i_{ac}\} \tag{2.8}$$

where $T_e$- Electromagnetic torque

$T_l$- Load torque

$\theta_e = \frac{P}{2}\theta_m$

$\theta_m$- rotor mechanical angle

$J$- Moment of inertia

$B$- Friction co-efficient

### 2.2.2 Steady state model

From Figure 2.1, steady state circuit is derived, which is shown in Figure 2.2.

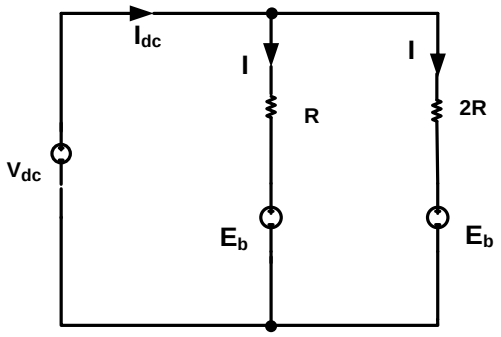


Figure 2.2: Equivalent circuit under steadystate

Electrical equations:

$$V_{dc} = \frac{2}{3} I_{dc} R + E_b \tag{2.9}$$

$$E_b = k_t \omega \tag{2.10}$$

where $V_{dc}$- dc source voltage

$I_{dc}$- steady state dc current

$E_b$- Average Back emf

Mechanical equations:

$$T_e = k_t \frac{I_{dc}}{3} \tag{2.11}$$

$$T_e = B\omega_m + T_l \tag{2.12}$$

From equation (2.9) and (2.10)

$$V_{dc} = \frac{2}{3} I_{dc} R + k_t \omega_m \tag{2.13}$$

$$V_{dc} = \frac{2RT_e}{k_t} + k_t \omega_m \tag{2.14}$$

$$\omega_m = \frac{V_{dc}}{k_t} - \frac{2RT_e}{k_t^2} \tag{2.15}$$

From equation (2.15), it can be observed that speed of the motor can be varied by varying the applied voltage to the motor. The analysis using transfer functions is done

below. Considering $60^\circ$ interval which is shown in Figure 2.1,equation (2.1) can be written as

$$V_{dc} = \frac{R}{2} i_{dc} + \frac{L}{2} \frac{di_{dc}}{dt} + k_t \omega_m \tag{2.16}$$

From Figure 1.8

$$V_{dc} - E_b = \frac{3}{2R(1 + s\tau_a)} I_{dc} \tag{2.17}$$

$$T_e = k_t \frac{I}{2} \tag{2.18}$$

$$I_{dc} = \frac{3I}{2} \tag{2.19}$$

$$therefore,\ T_e = \frac{k_t}{3} I_{dc} \tag{2.20}$$

where $\tau_a = \frac{L}{R}$ BLDC motor can be looked as as two-port network having two inputs $V_{dc}$ and $T_l$, two outputs $\omega_m$ and $I_{dc}$ which is shown in Figure 2.3. $T_l$ can be referred to as disturbance i/p.


Figure 2.3: BLDC motor

The outputs $\omega_m(s)$ and $I_{dc}(s)$ are related to the two inputs $V_{dc}(s)$ and $T_l(s)$ by the equations (2.21) and (2.22).

$$I_{dc}(s) = F_1(s) V_{dc}(s) + F_2(s) T_l(s) \tag{2.21}$$

$$\omega_m(s) = F_3(s) V_{dc}(s) + F_4(s) T_l(s) \tag{2.22}$$

where

$$F_1(s) = \frac{I_{dc}(s)}{V_{dc}(s)}\ when\ T_l(s) = 0$$

$$F_2(s) = \frac{I_{dc}(s)}{T_l(s)}\ when\ V_{dc}(s) = 0$$

$$F_3(s) = \frac{\omega_m(s)}{V_{dc}(s)}\ when\ T_l(s) = 0$$

$$F_4(s) = \frac{\omega_m(s)}{T_l(s)}\ when\ V_{dc}(s) = 0$$

The motor parameters used for simulation is given in Appendix A. Using equations (2.9) to (2.12) BLDC motor can be represented by the block diagram shown in Figure 2.4.

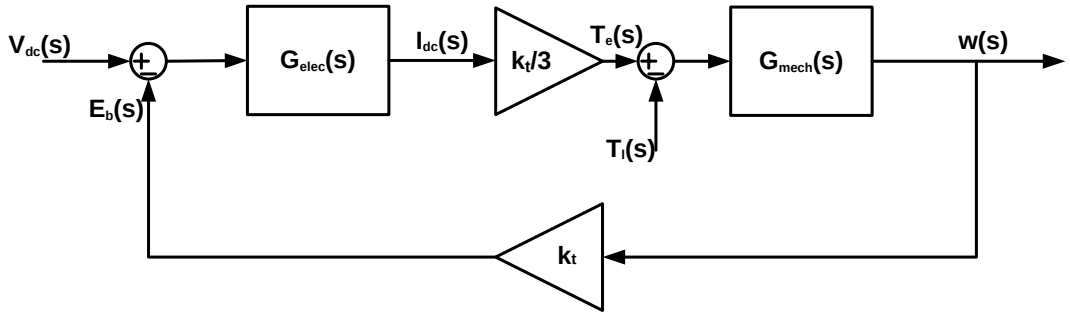


Figure 2.4: Block diagram of BLDC motor

where

$G_{elec}(s) = \frac{3}{2R(1+s\tau_a)}$

$G_{mech}(s) = \frac{1}{B(1+s\tau_m)}$

From Figure 2.4,

$$F_1(s) = \frac{I_{dc}(s)}{V_{dc}(s)}_{T_l=0} = \frac{\frac{3}{2R}(1+s\tau_m)}{(1+s\tau_a)(1+s\tau_m)+\frac{k_t^2}{2RB}} \tag{2.23}$$

By substituting the motor parameters given in Appendix A, steady state value of $I_{dc}(s)$ for step input of $V_{dc}(s) = \frac{24}{s}$ is $I_{dc}(s)$= 0.1461 A. Simulation result is shown in Figure 2.5. The average value of $I_{dc}$ from the figure is 0.15 A (approx).

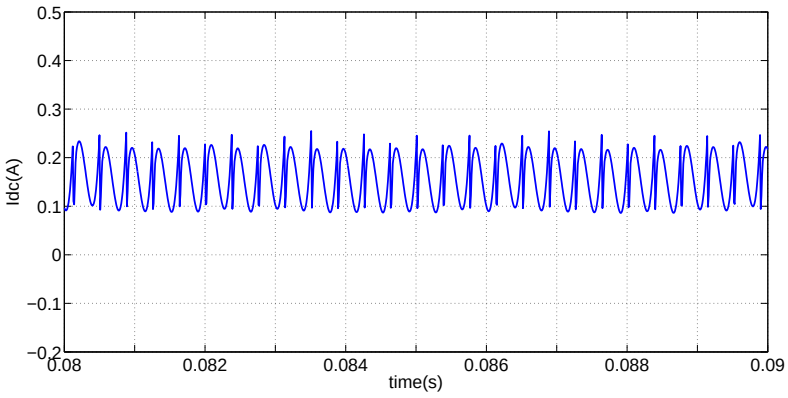


Figure 2.5: DC source current under no load for step change in $V_{dc}$ for $T_l$=0

The response $I_{dc}(s)$ to $T_l(s)$ for $V_{dc}$=0 is given by equation (2.24).

$$F_2(s) = \frac{I_{dc}(s)}{T_l(s)}_{V_{dc}=0} = \frac{\frac{3k_t}{2RB}}{(1+s\tau_a)(1+s\tau_m)+\frac{k_t^2}{2RB}} \tag{2.24}$$

The response $\omega_m(s)$ to $V_{dc}(s)$ for $T_l$=0 is given by equation (2.25).

$$F_3(s) = \frac{\omega_m(s)}{V_{dc}(s)}_{T_l=0} = \frac{\frac{k_t}{2RB}}{(1+s\tau_a)(1+s\tau_m)+\frac{k_t^2}{2RB}} \tag{2.25}$$

Steady state value of $\omega_m(s)$ for step input of $V_{dc}(s) = \frac{24}{s}$ is $\omega_m(s)$= 672 rad/s or 6417 rpm. Simulation result is shown in Figure 2.6.

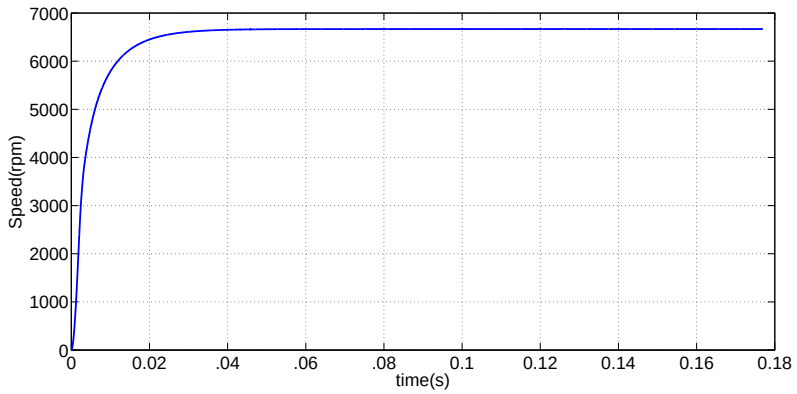


Figure 2.6: Speed response for step change in $V_{dc}$ for $T_l$=0

The transfer function $\omega_m(s)$ to $V_{dc}(s)$ for $T_l$=0 is given by equation (2.26).

$$F_4(s) = \frac{\omega_m(s)}{V_{dc}(s)}_{T_l=0} = \frac{\frac{-1}{B}(1+s\tau_m)}{(1+s\tau_a)(1+s\tau_m)+\frac{k_t^2}{2RB}} \tag{2.26}$$

The following figures show simulation results which gives an insight about the performance of BLDC motor.

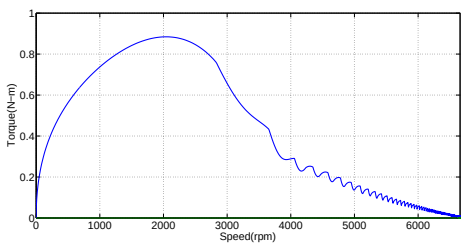


a)Speed-torque characteristics

Scale: x-axis- 1000 rpm/div , y-axis- 0.2 N-m/div

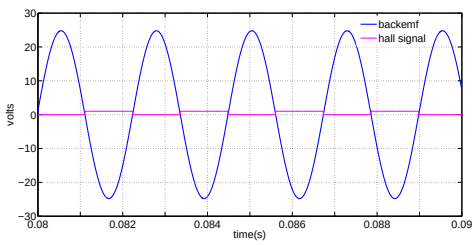


b) Back emf and hall sensor signals

Scale: x-axis- 2 ms/div , y-axis- 10 V/div

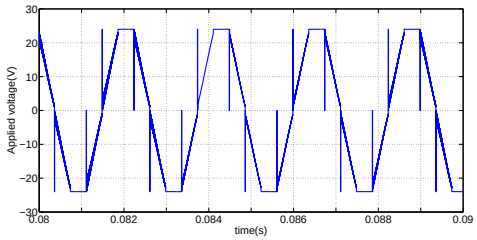


c) Applied voltage to motor

Scale: x-axis- 2 ms/div , y-axis- 10 V/div

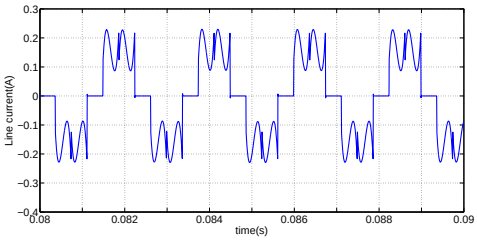


d) Motor line current

Scale: x-axis- 2 ms/div , y-axis- 0.1 A/div

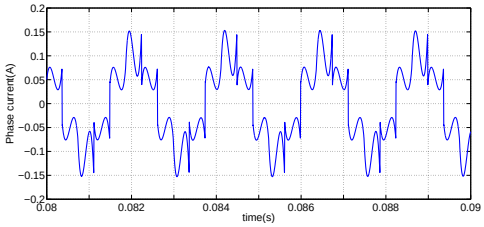


e) Motor phase current

Scale: x-axis- 2 ms/div , y-axis- 0.05 A/div

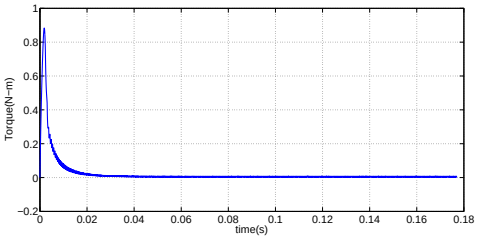


f) Torque vs time

Scale: x-axis- 20 ms/div , y-axis- 0.2 N-m/div

Figure 2.13: Open loop simulation results

**Observations**

- Figure 2.13 a) shows Speed-torque characteristics for free accleration.
- Figure 2.13 b) shows back emf and hall sensor signal generated from matlab code, which is given in Appendix A.
- Figure 2.13 c) shows applied voltage to motor under no load for full dc voltage.
- Figure 2.13 d) and e) shows motor line current and phase current respectively, under no load for full dc voltage.
- Figure 2.13 f) shows Torque response under no load.

## 2.3 Design of controller

Block diagram of BLDC drive is shown in Figure 2.14

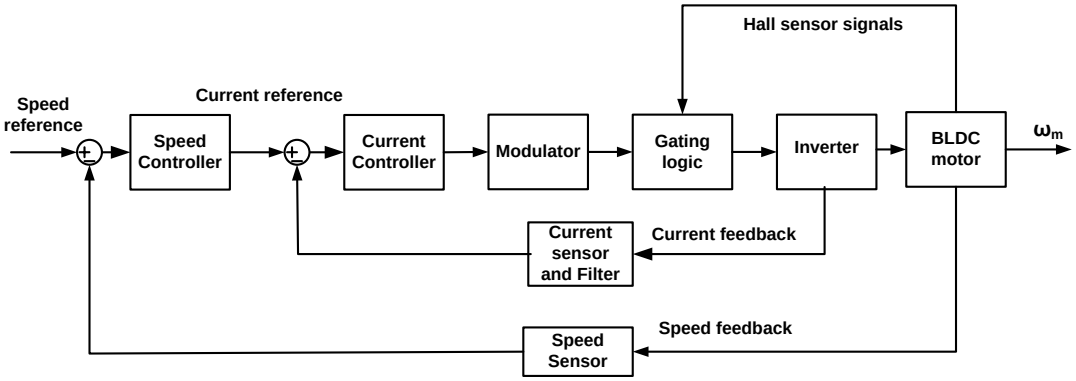


Figure 2.14: Block diagram of BLDC drive

For $T_l = 0$, from Figure 2.4

$$\frac{I_{dc}(s)}{V_{dc}(s)} = \frac{\frac{3}{2R}(1 + s\tau_m)}{(1 + s\tau_a)(1 + s\tau_m) + \frac{k_t^2}{2RB}} \tag{2.27}$$

$$= \frac{\frac{3}{2R}(1 + s\tau_m)}{s^2\tau_a\tau_m + s(\tau_a + \tau_m) + (\frac{k_t^2}{2RB} + 1)} \tag{2.28}$$

Characteristic equation of the above transfer function is

$$s^2\tau_a\tau_m + s(\tau_a + \tau_m) + (\frac{k_t^2}{2RB} + 1) = 0 \tag{2.29}$$

By substituting the machine parameters $\tau_a$ = 1.5e-3, $\tau_m$ = 0.6233, $k_t$ = 0.0353, $R$ = 0.8 ohm and $B$ = 7.7e-6 N-m-s/rad in equation (2.29), we get

$$s^2(9.3495e - 4) + s(0.6248) + 102.143 = 0 \tag{2.30}$$

The above equation can be written as

$$(1 + sT_1)(1 + sT_2) = 0 \tag{2.31}$$

By solving equation (2.31), $T_1 = 3.3363e - 3$ and $T_2 = 2.7129e - 3$

Therefore

$$\frac{I_{dc}(s)}{V_{dc}(s)} = \frac{K_1(1+s\tau_m)}{(1+sT_1)(1+sT_2)} \tag{2.32}$$

where

$K_1 = 1.697e-5$

$\tau_m = 0.6233$

The design of control loops starts from the inner loop which is the fastest loop and proceeds to the slowest loop which is the speed loop in this case. The design of current and speed controllers is explained in the following sections.

### 2.3.1 Current controller

PI controller is choosen as current controller as we require steady state error to be zero. Transfer function of current controller, $I_{cont}(s) = \frac{K_c(1+sT_c)}{sT_c}$ . Inner loop is shown in Figure 2.15. $H_c(s)$ is the tansfer function of current sensor and filter.

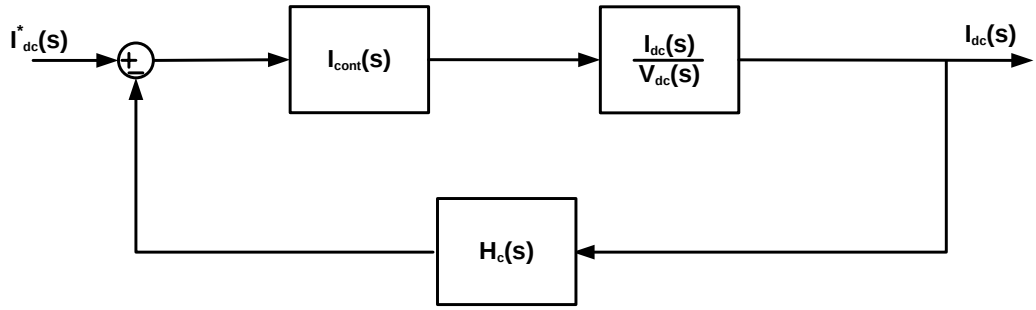


Figure 2.15: Current loop

where

$H_c(s) = \frac{1}{1+sT_f}$

$T_f = 1e-3$ (chosen to be 1/10$^{th}$ of switching frequency 10 kHz)

Loop transfer function of the innerloop, $I_{cont}(s) \times \frac{I_{dc}(s)}{V_{dc}(s)} \times H_c(s)$ is given by equation (2.33).

$$GH(s) = \frac{K_1K_c(1+sT_c)(1+s\tau_m)}{sT_c(1+sT_1)(1+sT_2)(1+sT_f)} \tag{2.33}$$

The following approximation can be done

$(1 + s\tau_m) \approx s\tau_m$, as $\tau_m$ is large. This reduces the loopgain transfer function to

$$GH(s) = \frac{K_1 K_c \tau_m (1 + sT_c)}{T_c(1 + sT_1)(1 + sT_2)(1 + sT_f)} \tag{2.34}$$

The equation (2.34) can be reduced to second order by judiciously choosing $T_c = T_2$. Therefore

$$GH(s) = \frac{\frac{K_1 K_c \tau_m}{T_c}}{(1 + sT_1)(1 + sT_f)} \tag{2.35}$$

Closed loop transfer function

$$\frac{I_{dc}(s)}{I^*_{dc}(s)} = \frac{K_1 K_c \tau_m (1 + sT_f)}{K_1 K_c \tau_m + T_c(1 + sT_1)(1 + sT_f)} \tag{2.36}$$

From equation (2.36),

characteristic equation: $s^2 T_1 T_f + s(T_1 + T_f) + (\frac{K_1 K_c \tau_m}{T_c} + 1) = 0$

$$T_1 T_f (s^2 + s\frac{(T_1 + T_f)}{T_1 T_f} + \frac{(\frac{K_1 K_c \tau_m}{T_c} + 1)}{T_1 T_f}) = 0 \tag{2.37}$$

$$s^2 + s\frac{(T_1 + T_f)}{T_1 T_f} + \frac{(\frac{K_1 K_c \tau_m}{T_c} + 1)}{T_1 T_f} = 0 \tag{2.38}$$

The equation (2.38) is in the standard second order form

$$s^2 + 2\zeta\omega_n s + \omega_n^2 = 0 \tag{2.39}$$

where

$$\omega_n^2 = \frac{(\frac{K_1 K_c \tau_m}{T_c} + 1)}{T_1 T_f} \tag{2.40}$$

$$2\zeta\omega_n = \frac{(T_1 + T_f)}{T_1 T_f} \tag{2.41}$$

where $\omega_n$ and $\zeta$ are natural frequency and damping ratio respectively. For good dynamic performance $\zeta = 0.707$ is chosen. By solving equations (2.40) and (2.41), we get $K_c = 0.007$. With this value of $K_c$, time taken for the current to settle is more. So $K_c = 1$ is chosen.

Therefore

$$I_{cont}(s) = \frac{1 + sT_2}{sT_2} \tag{2.42}$$

$$\frac{I_{dc}(s)}{I^*_{dc}(s)} = \frac{\tau_m(1 + sT_f)}{\tau_m + (1 + sT_1)(1 + sT_f)T_2} \tag{2.43}$$

From equation (2.44), characteristic equation is, $\tau_m + (1 + sT_1)(1 + sT_f)T_2 = 0$

By solving the above equation, $s = -649.944 \pm j8291.492$

For any second order system it takes five time constants to settle. From the above result time constant, $T_c = \frac{-1}{-649.944}s$. Therefore settling time, $T_s = 5T_c \approx 7.69ms$. Figure 2.17 shows for a current reference of 0.1 A, the actual current gets settled around $8ms$.

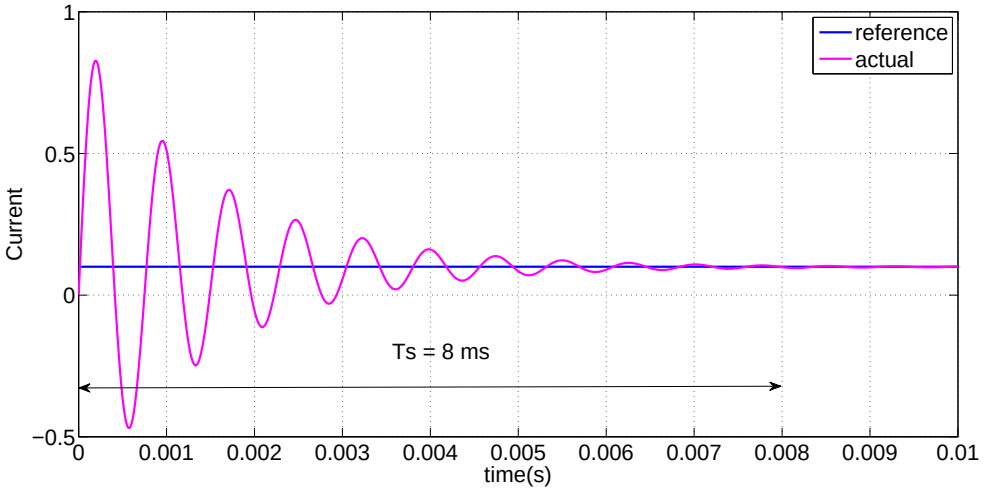


Figure 2.16: DC current response for a step input

Scale: x-axis- 1 ms/div , y-axis- 0.5 A/div

#### 2.3.1.1 First order approximation of Current loop

From Figure 2.15,

$$I_{cont}(s) \times \frac{I_{dc}(s)}{V^(_{dc}s)} = \frac{K_1(1 + s\tau_m)}{sT_2(1 + sT_1)} \tag{2.44}$$

$$1 + s\tau_m \approx s\tau_m$$

$$I_{cont}(s) \times \frac{I_{dc}(s)}{V^(_{dc}s)} = \frac{K'}{1 + sT_1} \tag{2.45}$$

where $K' = \frac{K_1 \tau_m}{T_2}$

$$\begin{aligned}\frac{I_{dc}(s)}{I^*_{dc}(s)} &= \frac{K'(1+sT_f)}{(1+sT_1)+K'(1+sT_f)} \\ &= \frac{K'(1+sT_f)}{1+K'+s(K'T_f+T_1)} \\ &= \frac{K'(1+sT_f)}{1+K'(1+\frac{s(K'T_f+T_1)}{1+K'}}\end{aligned}$$

$$\frac{I_{dc}(s)}{I^*_{dc}(s)} = \frac{K_i(1+sT_f)}{1+sT_i} \tag{2.46}$$

$$where\, K_i = \frac{K'}{1+K'} = 7e-3$$

$$T_i = \frac{T_1 + K'T_f}{1+K'} = 3.32e-3$$

### 2.3.2 Design of speed controller

From the approximation of inner current overall closed loop block diagram is shown in Figure 2.18.

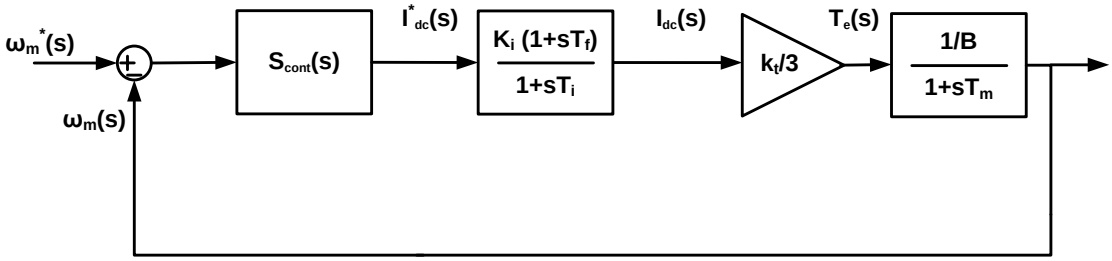


Figure 2.18: Speed loop

where

$$S_{cont}(s) = \frac{K_s(1+sT_s)}{sT_s}$$

From Figure 2.18,

$$\frac{\omega(s)}{\omega^*(s)} = \frac{K_f(1+sT_f)(1+sT_s)}{s(1+sT_i)(1+s\tau_m)+K_f(1+sT_f)(1+sT_s)} \tag{2.47}$$

where

$$K_f = \frac{K_s K_i k_t}{BT_s} \tag{2.48}$$

$$With\ T_f = 0,\ \frac{\omega_m(s)}{\omega_m^*(s)} = \frac{K_f + K_f T_s s}{T_i\tau_m s^3 + (T_i+\tau_m)s^2 + (K_f T_s + 1)s + K_f} \tag{2.49}$$

The above equation is written as,

$$\frac{\omega_m(s)}{\omega_m^*(s)} = \frac{a_0 + a_4 s}{a_3 s^3 + a_2 s^2 + a_1 s + a_0} \tag{2.50}$$

where

$$\begin{aligned} a_0 &= K_f \\ a_1 &= (K_f T_s + 1) \\ a_2 &= (T_i + \tau_m) \\ a_3 &= T_i \tau_m \\ a_4 &= K_f T_s \end{aligned}$$

Its magnitude is given by

$$\left|\frac{\omega_m(j\omega)}{\omega_m^*(j\omega)}\right| = \sqrt{\frac{a_0^2 + a_4^2\omega^2}{a_0^2 + (a_1^2 - 2a_0a_2)w^2 + (a_2^2 - 2a_1a_3)w^4 + a_3^2 w^6}} \tag{2.51}$$

For optimization, co-efficients of $\omega^2$ and $\omega^4$ are made equal to zero which results in

$$a_0^2 = 2a_1a_2 \tag{2.52}$$

$$a_2^2 = 2a_1a_3 \tag{2.53}$$

By solving equations (2.53) and (2.54) the values of $K_s$ and $T_s$ are obtained.

$$K_s = 8.724, T_s = 13.07e - 3$$

By solving the characteristic equation of equation (2.50), the roots of the equation are

$$s_1 = -151.535 s_2 = -75.663 \pm j131$$

Time constant,$T_c = \frac{-1}{-75.663} s$. Therefore settling time,$T_s = 5T_c \approx 66ms$.

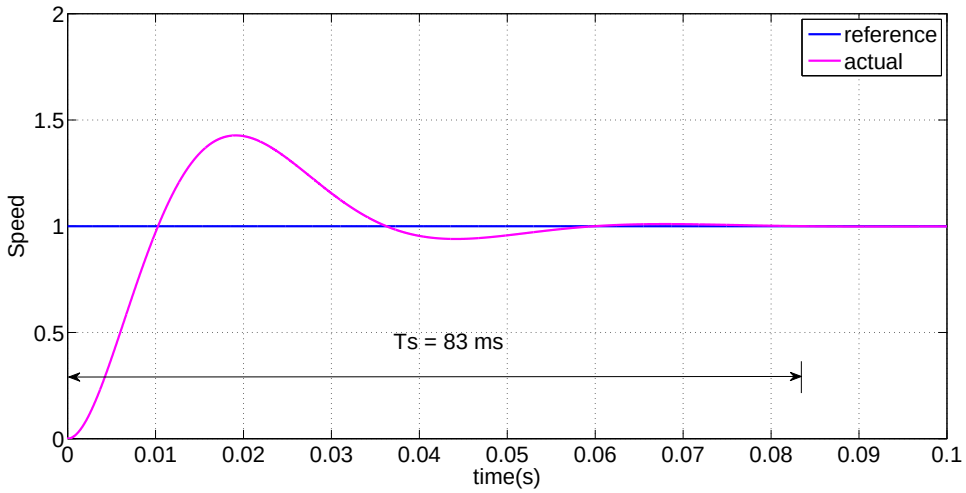


Figure 2.19: Speed response for step i/p
Scale: x-axis- 10 ms/div , y-axis- 0.5 (rad/s)/div

Figure shows speed response for a step input, settling time from simulation is $83ms$. Now with the designed values of current and speed controller, the simulation results are given in the next sections.

## 2.4 Closed loop (PWM control)

Block diagram for PWM mode of control is shown in Figure 2.14. Figure 2.29 shows simulation results for PWM mode of control.

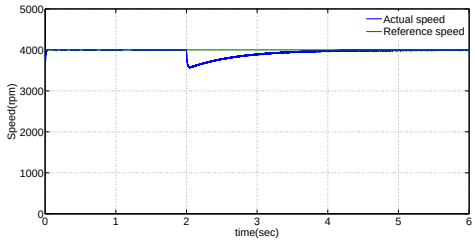


a) Speed vs time

Scale: x-axis- 1 s/div , y-axis- 1000 rpm/div

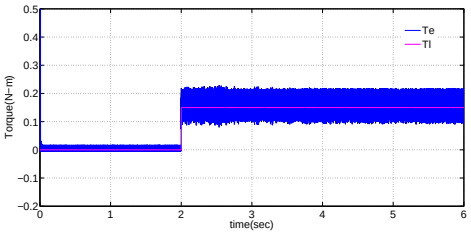


b) Torque vs time

Scale: x-axis- 1 s/div , y-axis- 0.1 N-m/div

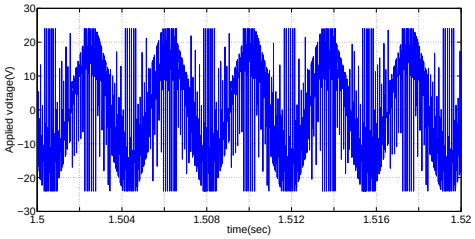


c) Applied voltage to motor

Scale: x-axis- 2 ms/div , y-axis- 10 V/div

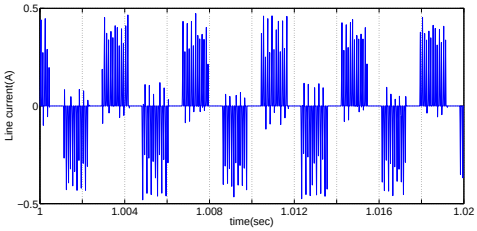


d) Motor Line current

Scale: x-axis- 2 ms/div , y-axis- 0.5 A/div

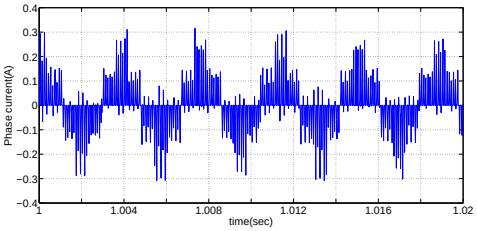


e) Motor phase current

Scale: x-axis- 2 ms/div , y-axis- 0.1 A/div

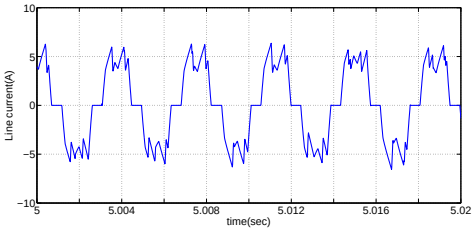


f) Motor line current under load

Scale: x-axis- 2 ms/div , y-axis- 5 A/div

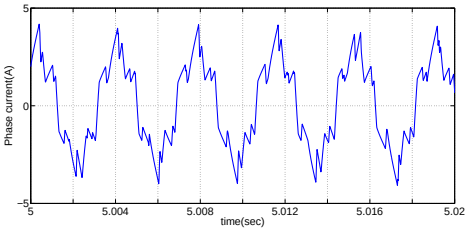


g) Motor phase current under load

Scale: x-axis- 2 ms/div , y-axis- 5 A/div

Figure 2.29: Simulation results for PWM control

**Observations:**

- Figure 2.29 a) and b) shows Speed response and Torque response respectively, for a speed reference of 4000 rpm under no load. At t=2 sec load of 0.15 N-m is applied. Speed falls momentarily and gets settled to 4000 rpm.
- Figure 2.29 c) shows Applied voltage to motor for speed reference of 4000 rpm.
- Figure 2.29 d) and e) shows motor line current and phase current respectively for a speed reference of 4000 rpm.
- Figure 2.29 f) and g) shows motor line current and phase current respectively for a load of 0.15 N-m.

## 2.5 Closed loop(DC-link voltage control)

In DC-Link voltage control mode DC voltage applied is varied. DC-DC converter is used for varying the DC voltage. It is designed for 1% voltage ripple and 10% current ripple is shown in Appendix A. Block diagram of DC-Link voltage control mode is shown in Figure 2.30.

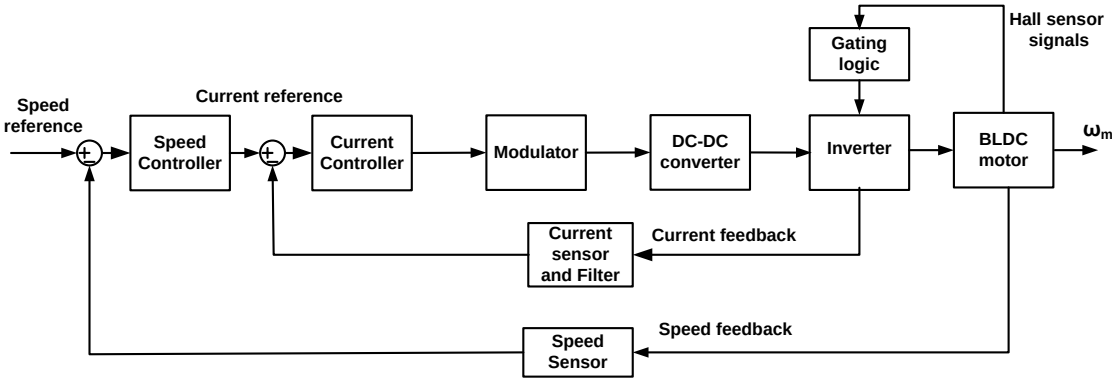


Figure 2.30: Block diagram of DC-Link voltage control mode

The following figure shows simulation results of DC-Link voltage mode of control.

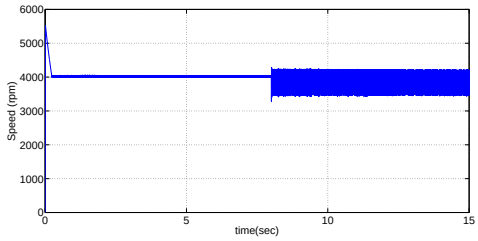


a) Speed vs time

Scale: x-axis- 5 s/div , y-axis- 1000 rpm/div

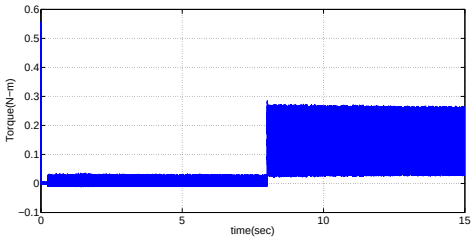


b) Torque vs time

Scale: x-axis- 5 s/div , y-axis- 0.1 N-m/div

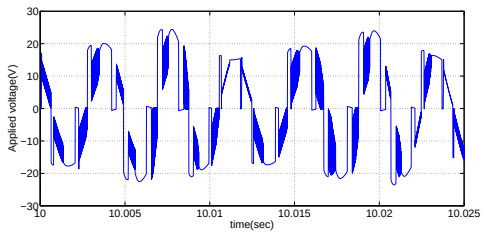


c) Motor applied voltage

Scale: x-axis- 5 ms/div , y-axis- 10 V/div

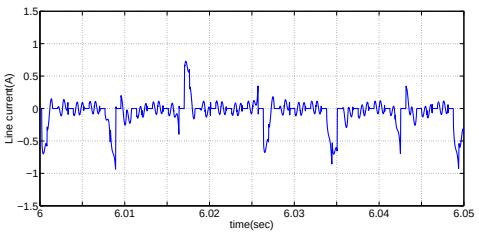


d) Motor Line current

Scale: x-axis- 5 ms/div , y-axis- 0.5 A/div

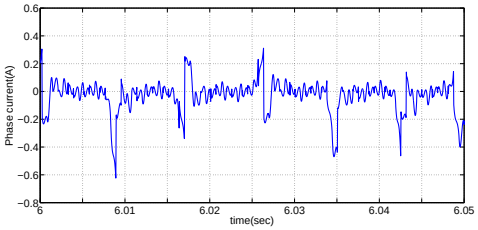


e) Phase current

Scale: x-axis- 5 ms/div , y-axis- 0.2 A/div

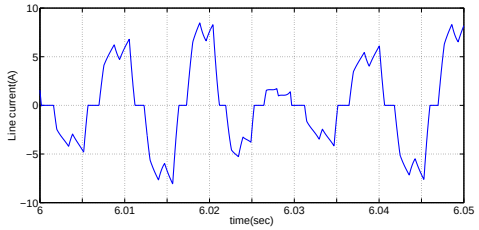


f) Line current with load

Scale: x-axis- 5 ms/div , y-axis- 5 A/div

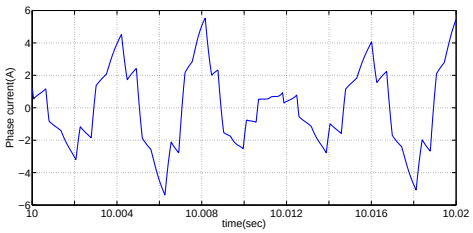


g) Phase current with load

Scale: x-axis- 2 ms/div , y-axis- 2 A/div

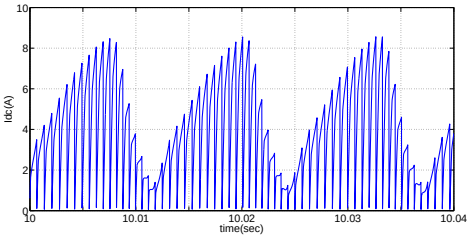


h) DC source current

Scale: x-axis- 10 ms/div , y-axis- 2 A/div

Figure 2.39: Simulation results for DC-Link mode of control

## Observations

- Figure 2.39 a) and b) shows Speed response and Torque response respectively, for a speed reference of 4000 rpm under no load. At t=8 sec load of 0.15 N-m is applied.
- Figure 2.39 c) shows Applied voltage to motor for speed reference of 4000 rpm. Due to ripple in DC voltage applied voltage to motor is not uniform.
- Figure 2.39 d) and e) shows motor line current and phase current respectively for a speed reference of 4000rpm under no load.
- Figure 2.39 f) and g) shows motor line current and phase current respectively for a speed reference of 4000rpm and for a load of 0.15 N-m. Line current and phase current are not uniform beacause of ripple in DC voltage.

- Figure 2.39 h) shows DC source current for a load of 0.15 N-m.

The next section compares torque ripple in PWM control and DC-Link voltage control.

## 2.6 Torque ripple comparison

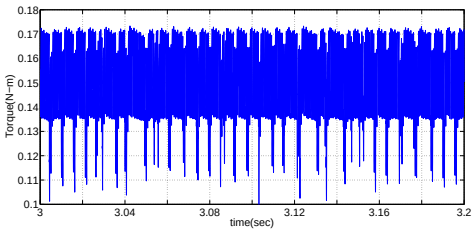


a) Torque in PWM control
Scale: x-axis- 20 ms/div , y-axis- 0.01 N-m/div

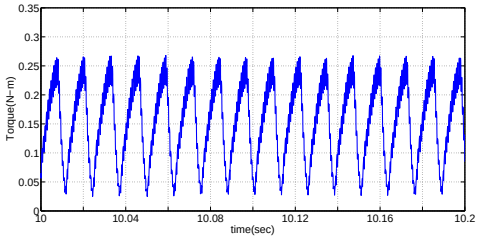


b) Torque in DC-Link voltage control
Scale: x-axis- 20 ms/div , y-axis- 0.05 N-m/div

Figure 2.41 a) shows torque in PWM mode of control. Torque ripple = 39%(approx.).

Figure 2.41 b) shows torque in DC-Link volatge mode of control. Torque ripple = 150%(approx.).

**Observation:** The ripple in DC-Link voltage control is more than the PWM control. This is one of the disadvantages in DC-Link control. This is due to ripple in DC voltage.

# CHAPTER 3

# HARDWARE

## 3.1 Hardware implementation

Block diagram of control scheme is shown in Figure 3.1.

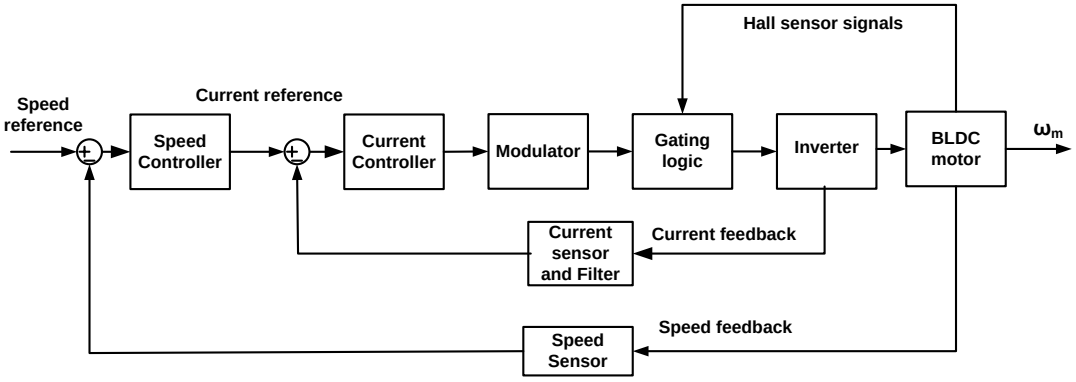


Figure 3.1: Block diagram of the drive for BLDC in PWM control mode

The drive of a BLDC motor consists of speed controller, current controller, speed sensor, current sensor, modulator, inverter and gating logic for inverter. The detailed explanation is given below.

The Figure 3.2 is a frequency to voltage converter circuit which is a speed sensor. It converts hall signal frequency which is directly proportional to speed, to voltage which can be used as speed feedback.

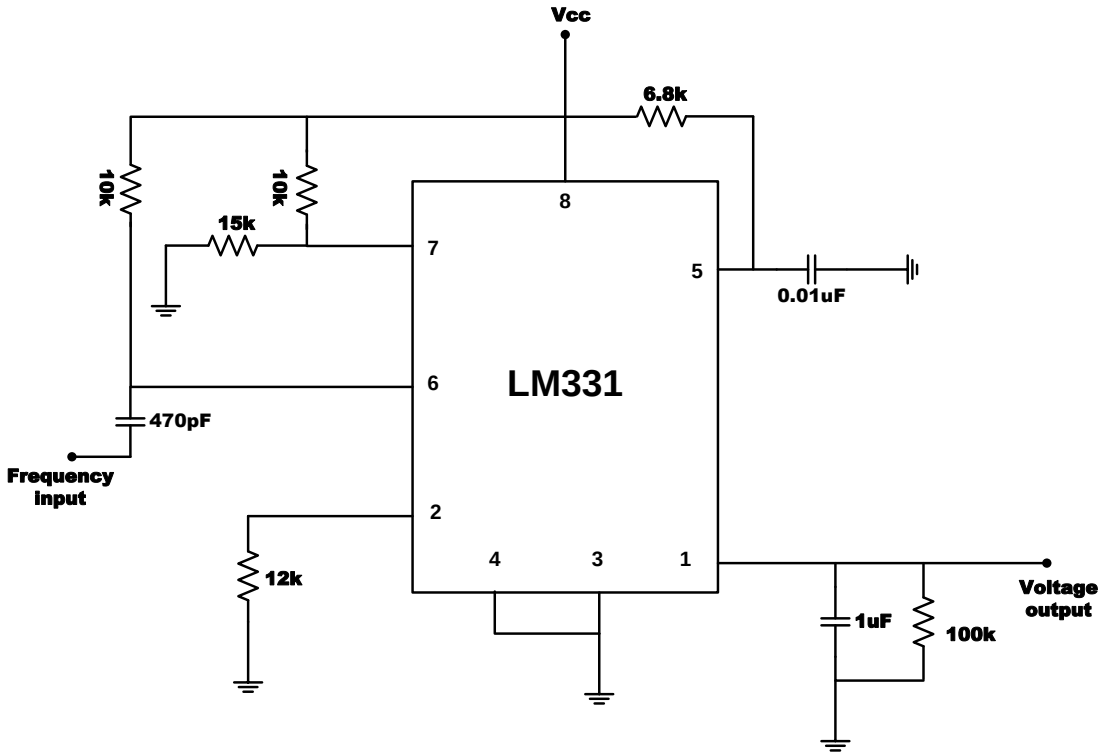


Figure 3.2: Frequency to voltage converter

The speed reference is compared with the output signal from LM331 and the error is processed through PI controller which is implemented using LM318. It is shown in Figure 3.3.

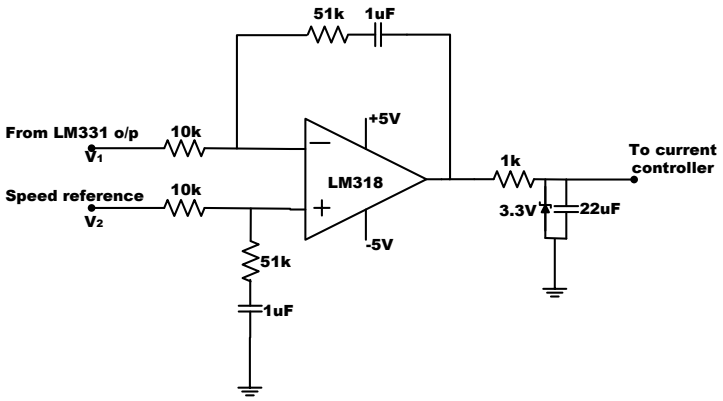


Figure 3.3: Speed controller

The output of the speed controller is given as reference signal to the current controller. It is compared with the amplified signal from current sensor and the error is processed

through PI controller. It is implemented using LM318 which is shown in Figure 3.4. The current sensor used is $LEM\ LA-55P$.

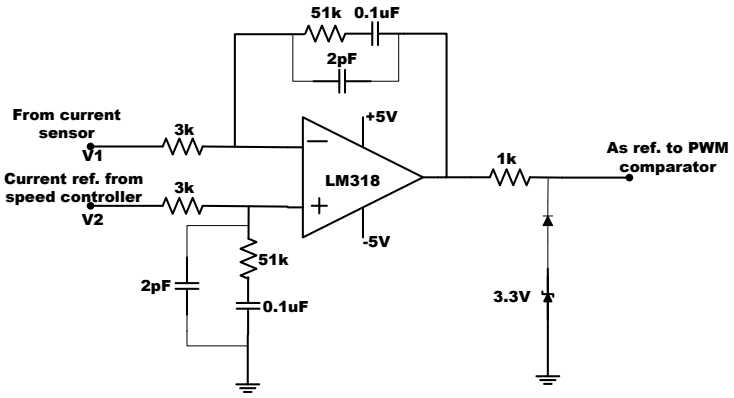


Figure 3.4: current controller

The following picture shows the current controller, speed sensor, current sensor and current controller.

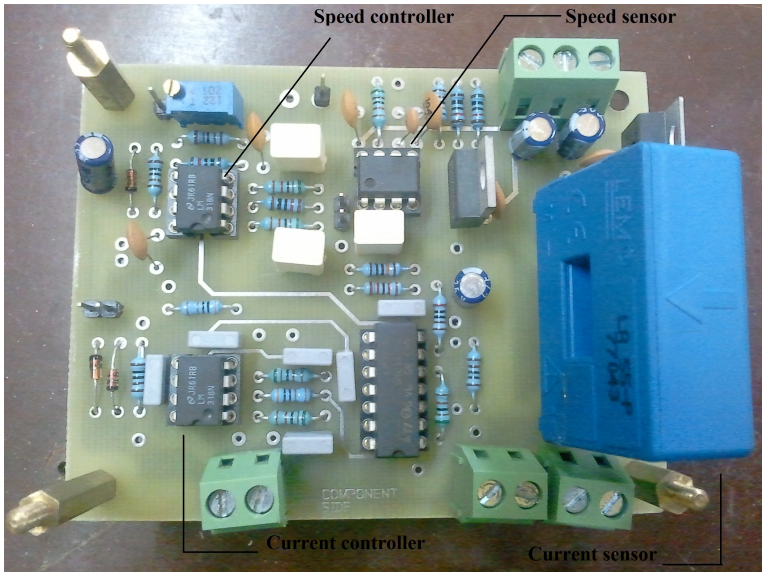


Figure 3.5: Controllers and sensors

The MOSFETś $(IRF540)$ are used as switches in the inverter. The inverter built is shown in Figure 3.6.

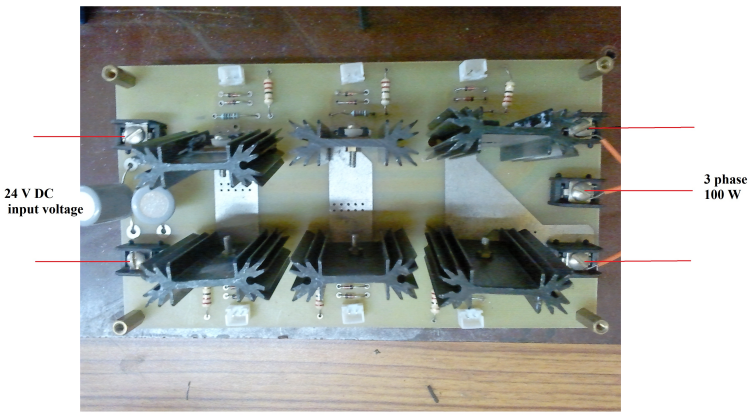


Figure 3.6: 3-phase Inverter

The gate drive circuit which is built using IR 2110ś is shown in Figure 3.7. As IR 2110 is capable of driving the high side switch and low side switch, each IR 2110 is used for driving one leg of the inverter.

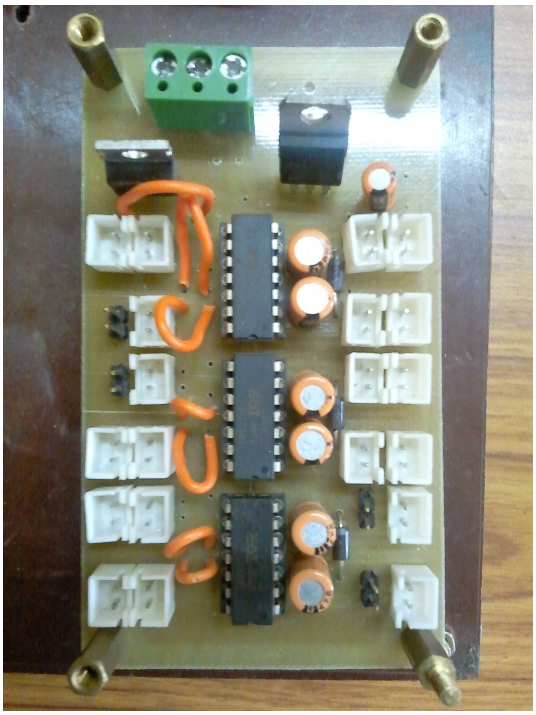

Figure 3.7: Gate drive circuit for inverter

The switching signals to the inverter are ANDed with the pulses from modulator. TL494 is used as pulse-width modulator. The carrier signal which is sawtooth is generated internally by the IC. By varying the values of resistance and capacitance of the $6^{th}$ and

$5^{th}$ pin the frequency of the carrier signal can be varied. It is set at 10 kHz. This carrier signal is compared with the reference signal which is the output of current controller. The following figure shows the implementation.

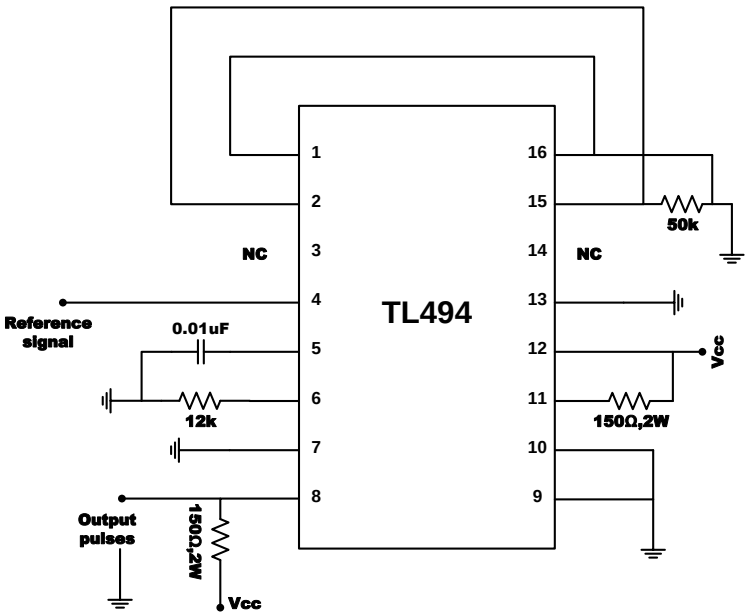


Figure 3.8: Modulator

Hardware setup of modulator along with AND gates is shown in Figure 3.9.

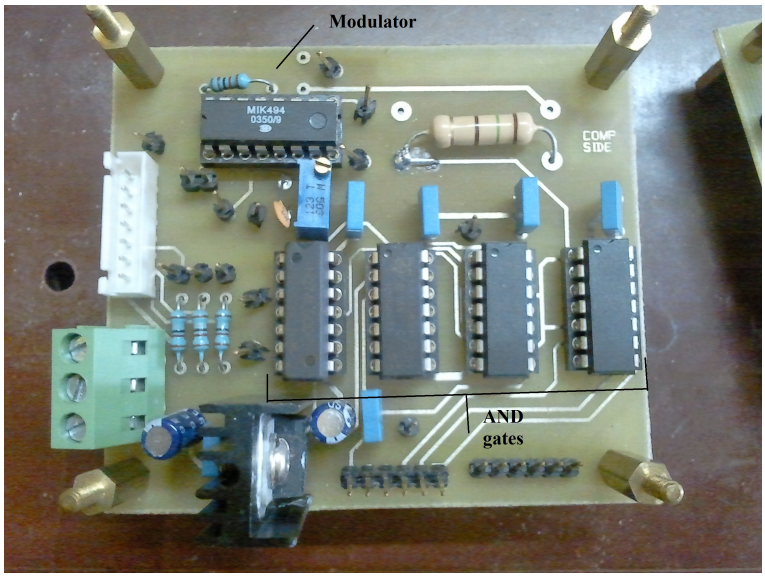


Figure 3.9: Modulator and AND gates

The overall hardware setup is shown in Figure 3.10.

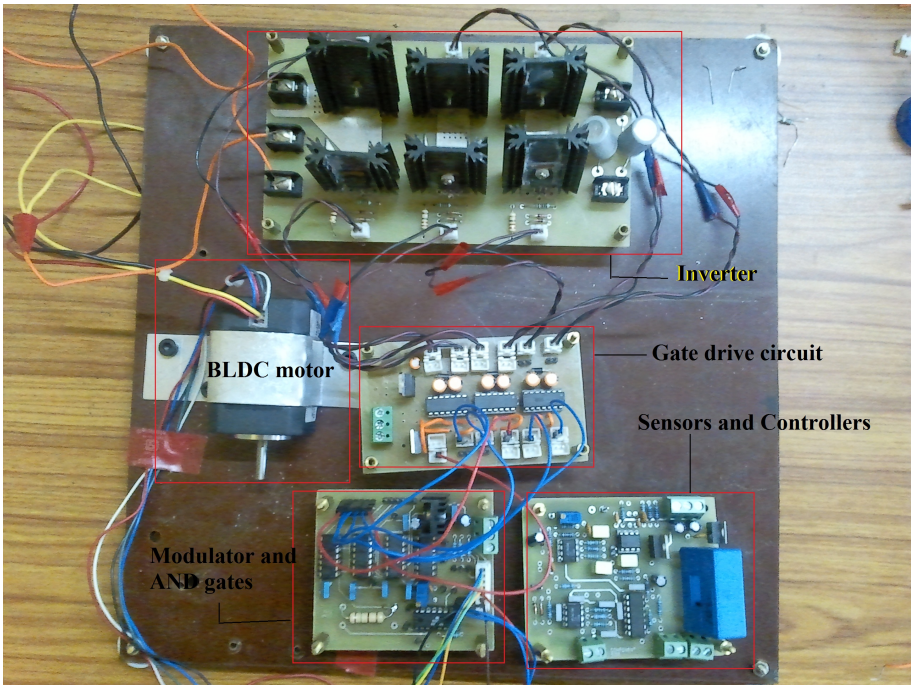


Figure 3.10: Hardware setup

## 3.2 Experimental results

This section presents the Experimental results of BLDC motor drive for PWM mode of control under no load.

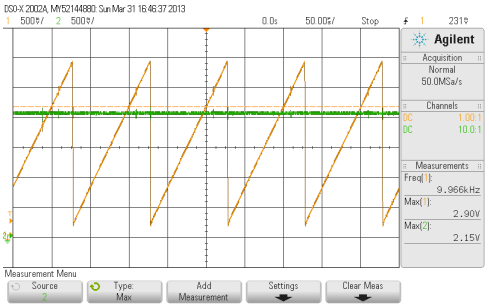


a) PWM carrier wave
Scale: x-axis- 50 $\mu$s/div , y-axis- 500 mV/div

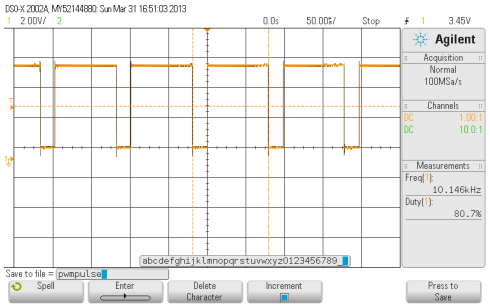


b) Pulses from modulator
Scale: x-axis- 50 $\mu$s/div , y-axis- 2 V/div

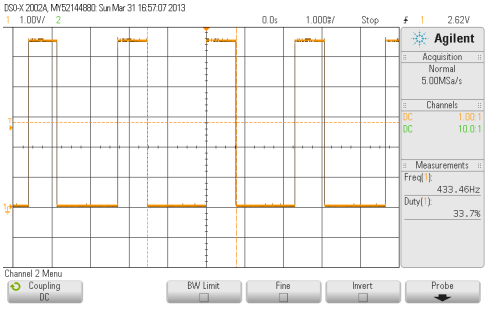


c) Switching signal to gate

Scale: x-axis- 1 ms/div , y-axis- 1 V/div

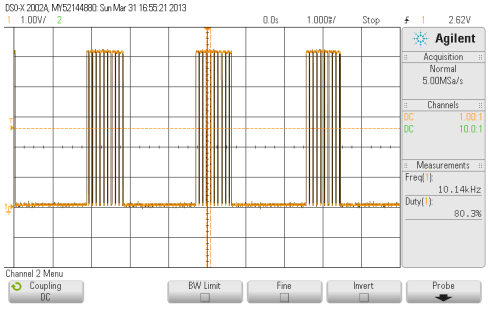


d) Switching signal to gate with PWM

Scale: x-axis- 1 ms/div , y-axis- 1 V/div

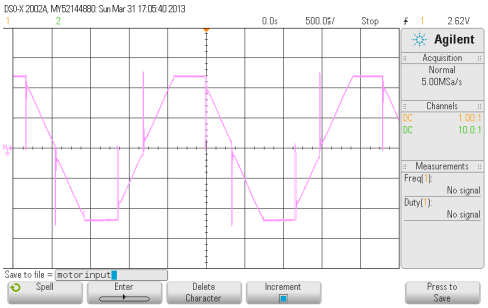


e) Applied voltage to motor

Scale: x-axis- 500 $\mu$s/div , y-axis- 10 V/div

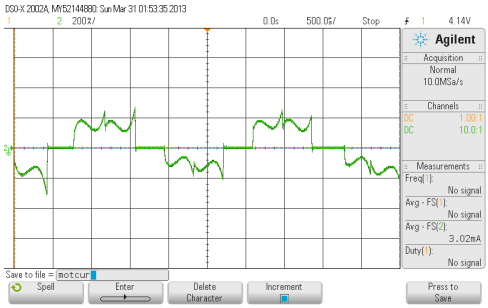


f) Motor line current

Scale: x-axis- 500 $\mu$s/div , y-axis- 0.2 A/div

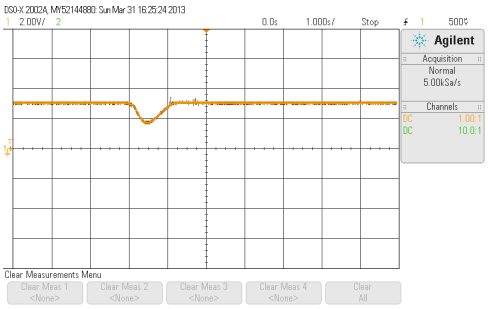


g) Speed vs time

Scale: x-axis- 1 s/div , y-axis- 2 V/div

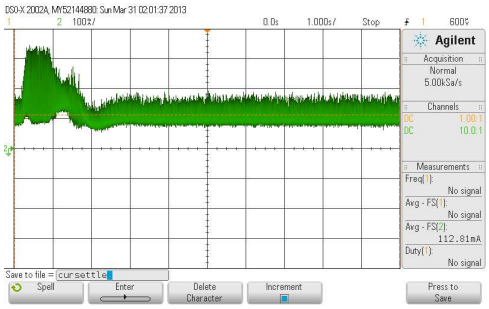


h) DC source current vs time

Scale: x-axis- 1 s/div , y-axis- 0.1 A/div

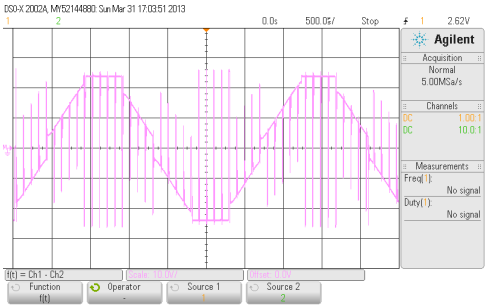


i) Applied voltage to motor(PWM)

Scale: x-axis- 500 $\mu$s/div , y-axis- 10 V/div

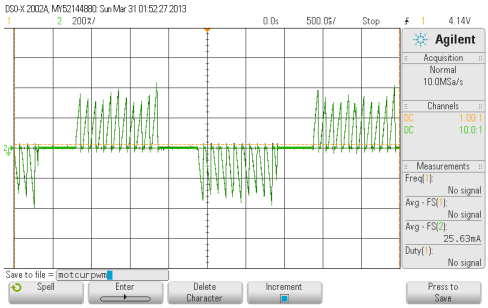


j) Motor line current

Scale: x-axis- 500 $\mu$s/div , y-axis- 0.2 A/div

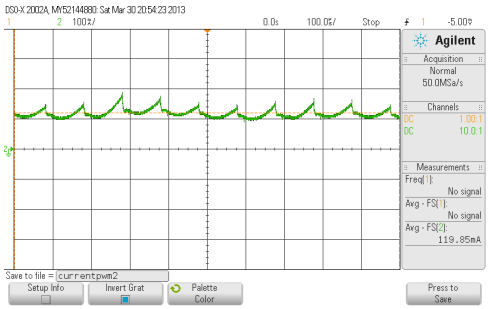


k) DC source current(PWM)
Scale: x-axis- 100 $\mu$s/div , y-axis- 0.1 A/div

Figure 3.23: Experimental waveforms of BLDC motor drive

## Observations

- Figure 3.23 a) shows PWM carrier wave used for generation of 10 kHz pulses. Its peak-peak amplitude is 3.3 V.
- Figure 3.23 b) shows pulses of frequency 10 kHz & amplitude 5 V, generated after comparing carrier wave with reference value.
- Figure 3.23 c) and d) shows switching signal of one of the switches without PWM and with PWM respectively which are gate of MOSFET.
- Figure 3.23 e) and f) shows applied voltage to motor and motor line current under no load for full dc voltage(i.e.without pwm).
- Figure 3.23 g) shows Speed response for a speed reference of 3 V which corresponds to 4870 rpm. At t=3 sec a disturbance is given by holding the motor shaft for an instant and then releasing it. It can be observed that speed is settled.
- Figure 3.23 h) shows DC current response for a speed reference of 3 V which corresponds to 4870 rpm. At t=0.2 sec a disturbance is given by holding the motor shaft for an instant and then releasing it. It can be observed that current is settled.
- Figure 3.23 i) and j) shows applied voltage to motor and motor line current under no load for speed reference of 4870 rpm.
- Figure 3.23 k) shows DC source current no load for speed reference of 4870 rpm.

# CHAPTER 4

# Conclusion

Modeling of BLDC motor is done. Simulation results of BLDC motor using the model equations are shown. Controller design is presented. Simulation results of PWM mode of control and DC-Link mode of control are shown. Hardware implementation in PWM mode of control is explained. Experimental results of BLDC drive for PWM mode of control are presented.

# APPENDIX A

## A.1 Code for Back emf and hall sensor signals

```
function out= newfunc( in )
phi=in;
kw=0.0355;
if phi<0
phi=-phi;
end
if (phi/(2*pi))>=1
n=floor(phi/(2*pi));
phi=phi-(n*2*pi);
end

if (phi>=0&&phi<(pi/3))
fa=sin(phi+(2*pi/3));
ha=0;

else if (phi>=(pi/3)&&phi<(4*pi/3))
fa=sin(phi+(2*pi/3));
ha=1;
else if (phi>=(4*pi/3)&&phi<(2*pi))
fa=sin(phi+(2*pi/3));
ha=0;
end
end
end
if (phi>=0&&phi<pi)
```

```
fb=sin(phi);
hb=0;


else if (phi>=(pi)&&phi<(2*pi))
fb=sin(phi);
hb=1;
end
end

if (phi>=0&&phi<(2*pi/3))
fc=sin(phi+(4*pi/3));
hc=1;

else if (phi>=(2*pi/3)&&phi<(5*pi/3))
fc=sin(phi+(4*pi/3));
hc=0;
else if (phi>=(5*pi/3)&&phi<(2*pi))
fc=sin(phi+(4*pi/3));
hc=1;


end
end
end
out(1)=kw*fa;
out(2)=kw*fb;
out(3)=kw*fc;
out(4)=ha;
out(5)=hb;
out(6)=hc;
end
```

## A.2 DC-DC converter(Buck)

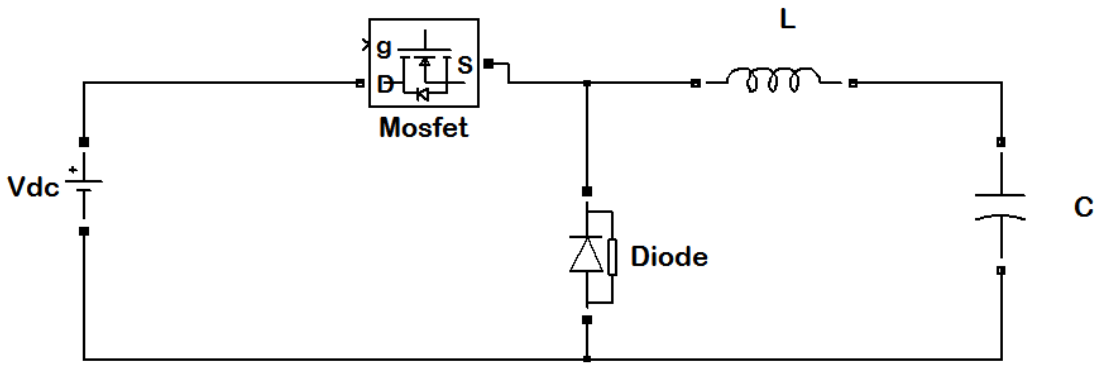


Figure A.1: simulink model of buck converter

## A.3 Motor parameters

Table A.1: Motor parameters

| *Parameter* | *Value* | *Units* |
|---|---|---|
| Rated power | 55 | W |
| Rated voltage | 24 | V |
| Peak torque | 0.38 | N-m |
| Rated speed | 4000 | rpm |
| Line to Line resistance | 0.8 | ohm |
| Line to Line inductance | 1.2 | mH |
| Torque constant | 0.0353 | N-m/A |
| Back emf constant | 0.0353 | V/rad/s |
| Moment of inertia | 47e-6 | kg-m$^2$ |
| Friction co-efficient | 7.7e-6 | N-m/rad/sec |

# REFERENCES


[1] T.J.E.Miller., *"Brushless permanent-magnet and reluctance motor drives",* Oxford University Press, New york, 1989.

[2] R. Krishnan., *"Electric Motor drives: Modelling, Analysis and Control",* Prentice Hall, Upper Saddle River, New Jersey, Third Edition, 2002.

[3] Bimal K.Bose., *"Modern power electronics and AC drives"* Prentice Hall, Upper Saddle River, New Jersey, 2005.

[4] Yedale Padmaraja., *"Brushless DC Motor Fundamental",* AN885, Microchip Technology Inc (2003).